PREDICTION OF EXTREME WAVE CONDITIONS IN THE BLACK SEA WITH NUMERICAL MODELS

Eugen Rusu, Liliana Rusu, and C. Guedes Soares
Unit of Marine Technology and Engineering,
Technical University of Lisbon, Av. Rovisco Pais, 1049-001 Lisboa, Portugal

1. INTRODUCTION

The Black Sea wave climate was the subject of various studies and research projects. In the last years this region becomes an important corridor for energy transportation. These new economical developments are leading to increased sea traffic and request the possibility of better prediction systems for the wave conditions especially concerning the nearshore areas in the neighborhood of the major ports.

Although in a closed sea the fetch is smaller than in open-ocean and the average wave conditions are considerably less energetic than for example on the Iberian coasts of the Atlantic Ocean, strong storms can generate sometimes in the Black Sea waves comparable in terms of wave heights with the big ocean waves. Freak waves have been also reported (Divinsky et al. 2004).

Various implementations of the WAM model have been performed in the Black Sea area, being calibrated either with in situ or remotely sensed data. The implementation of Vlachev et al. (2004) will be considered here as a reference because of the availability of the same wind data field.

The basic scientific philosophy of SWAN is identical to that of WAM (Cycle 3 and 4). SWAN is a third generation wave model and it uses the same formulations for the source terms (although SWAN uses the adapted code for the DIA technique). On the other hand, SWAN contains some additional formulations primarily for shallow water. Of course, SWAN is less efficient for oceanic scales than WAM. However, as regards the sub oceanic scales, as the present case is, it seems to be more effective.

The SWAN model was initially designed for coastal applications. However, in the last versions its capacities were substantially extended both in the offshore and nearshore directions. Thus high order propagation schemes associated to large areas (S&L and SORDUP) and parameterizations to counteract the Garden Sprinkler effect were included, so that the model can be used now successfully for large geographical domains. On the other hand, diffraction, which is relevant in high-resolution simulations, was also introduced in a phase-decoupled approach and this extends the applicability of the model in the nearshore direction. The multitude of options existent in SWAN make the model very flexible but at the same time render it quite confusing for an untrained operator to deal with all the various options.

The present work will present some steps in the implementation of a wave prediction system in the Black Sea based on SWAN. The system is first calibrated using in situ data from the east coast. In the second step using the measurements from the Gloria drilling unit, which is operating on the west coast, a validation of the model configuration is also made.

The major advantage brought by designing such a wave prediction system based on SWAN is that a single model can be used for generation, transformation and up to local areas for the entire sea. Since it is simpler to nest a wave model into itself than into another model this allows a better communication between various model domains leading to an increased flexibility of the model system.

2. DEEP WATER WAVE MODELING WITH SWAN

SWAN as most of the third generation wave models solves the action balance equation in all the five dimensions (time, geographical and wave number spaces). In deep water, three components are significant in the expression of the total source term:

$$S_{total} = S_{in} + S_{dis} + S_{nl} \qquad (1)$$

These correspond to the atmospheric input, white-cap dissipation and nonlinear quadruplet interactions, respectively.

Transfer of wind energy to the waves is described in SWAN with the resonance mechanism of Phillips (1957) and the feed-back mechanism of Miles (1957). The corresponding source term for these mechanisms is commonly described as the sum of linear and exponential growth:

$$S_{in}(\sigma, \theta) = A + BE(\sigma, \theta) \qquad (2)$$

in which A describes linear growth and BE exponential growth. The expression for the term A is due to Cavaleri and Malanotte-Rizzoli (1981) with a filter to avoid growth at frequencies lower than the Pierson-Moskowitz frequency, (Tolman, 1992). Two optional expressions for the coefficient B are used in the model. The first is taken from an early version of the WAM model, known as WAM Cycle 3, (the WAMDI group, 1988). It is due to Snyder et al. (1981), rescaled in terms of friction velocity by Komen et al. (1984), and it is currently called the Komen parameterization. The second expression is due to Janssen (1989, 1991) and it is based on the quasi-linear wind-wave theory.

White-capping is primarily controlled by the steepness of the waves. In the third generation wave models presently operating (including SWAN) the white-cap formulations are based on the pulse model of Hasselmann (1974), as adapted by the WAMDI group (1988), so as to be applicable in finite water depth. This expression is:

$$S_{ds,w}(\sigma,\theta) = -\Gamma \tilde{\sigma} \frac{k}{\tilde{k}} E(\sigma,\theta) \qquad (3)$$

where $\tilde{\sigma}$ and $\tilde{k}$ denote the mean frequency and the mean wave number, and the coefficient Γ depends on the overall wave steepness

$$\Gamma = \Gamma_{KJ} = C_{ds}\left((1-\delta)+\delta\frac{k}{\tilde{k}}\right)\left(\frac{\tilde{S}}{\tilde{S}_{PM}}\right)^p \qquad (4)$$

For δ=0 the expression of Γ reduces to the expression as used by the WAMDI group (1988). The coefficients C_{ds}, δ and p are tuneable coefficients, $\tilde{S}$ is the overall wave steepness and $\tilde{S}_{PM}$ is the value of this parameter for the Pierson-Moskowitz spectrum (= $(3.02\times10^{-3})^{1/2}$). The values of the tunable coefficients C_{ds}, δ and p in the SWAN model have been obtained by Komen et al. (1984) and Janssen (1992) by closing the energy balance of the waves in idealized wave growth conditions (both for growing and fully developed wind seas) for deep water. This implies that coefficients in the steepness dependent coefficient Γ depend on the wind input formulation that is used. Since two different wind input formulations are used in the SWAN model, two sets of coefficients are used. For the Komen parameterization (corresponding to WAM Cycle 3) C_{ds} = 2.36×10^{-5}, δ=0 and p = 4. The tuneable coefficients are in this case C_{ds} and $\tilde{S}_{PM}^2$. In the Janssen parameterization (being assumed also p = 4) C_{ds} = 4.10×10^{-5} and δ=0.5 (as used in the WAM cycle 4). The tuning parameters used in this case are δ and C_{ds1} (default 4.5) which is given by:

$$C_{ds1} = C_{ds}\left(\frac{1}{\tilde{S}_{PM}}\right)^4 \qquad (5)$$

An alternative formulation for white-capping is based on the Cumulative Steepness Method as described in Hurdle and Van Vledder. (2004). With this method dissipation due to white-capping depends on the steepness of the wave spectrum at and below a particular frequency. It is defined as (directionally dependent):

$$S_{st}(\sigma,\theta) = \int_0^\sigma \int_0^{2\pi} k^2 |\cos(\theta-\theta')|^m E(\sigma,\theta)d\sigma d\theta \quad (6)$$

In this expression the coefficient m controls the directional dependence. It is expected that this coefficient will be about 1 if the straining mechanism is dominant; m is more than 10 if other mechanism play a role (e.g. instability that occurs when vertical acceleration in the waves becomes greater than gravity). Default in SWAN is m = 2. The new white-capping source term is given by:

$$S_{wc}^{st}(\sigma,\theta) = -C_{wc}^{st}S_{st}(\sigma,\theta)E(\sigma,\theta) \qquad (7)$$

with C_{wc}^{st} a tuneable coefficient (with the default value 0.5).

In deep water, quadruplet wave-wave interactions dominate the evolution of the spectrum. They transfer wave energy from the spectral peak both to lower frequencies (thus moving the peak frequency to lower values) and to higher frequencies (where the energy is dissipated by white-cap). A full computation of the Boltzmann integral expressing the quadruplet wave-wave interactions is extremely time consuming and not convenient in any operational wave model. Nevertheless, the current version of SWAN (40.41) has two options to compute the Boltzmann integral in an exact manner. The first approach is the so-called FD-RIAM technique as proposed by Hashimoto et al. (1998). This approach enables to capture the frequency shift and the spectral shape changes as water depth decreases. The second approach is the exact method developed by Webb, Tracy and Resio, (Resio et al., 2001). This algorithm was reprogrammed by Van Vledder, bearing the name Xnl (Van Vledder and Bottema, 2003). This method is also enabling to capture the frequency shift and the spectral shape changes as water depth decreases.

A number of techniques, based on parametric methods or other types of approximations have been proposed to improve computational speed, as reviewed by Young and Van Vledder (1993). In SWAN, the computations are carried out with the Discrete Interaction Approximation (DIA) of Hasselmann et al. (1985). This

DIA has been found to be quite successful in describing the essential features of a developing wave spectrum. In some cases, the DIA technique may not be accurate enough. DIA uses the fact that the interactions between closely neighboring wave numbers reproduce the principal features of the nonlinear transfer. In each configuration two wave numbers are taken identical $\vec{k}_1 = \vec{k}_2 = \vec{k}$, while the wave numbers $\vec{k}_3$ and $\vec{k}_4$ are of different magnitude. The second quadruplet is the mirror of the first one at the $\vec{k}$ axis. The computation of the S_{nl} source term is identical to that of the exact Boltzmann integral but is taken over a 2D continuum. DIA uses the fact that the interactions between closely neighboring wave numbers reproduce the principal features of the nonlinear transfer. In each configuration two wave numbers are taken identical

In SWAN the quadruplets can be integrated by four different DIA numerical procedures: semi-implicit computation of the nonlinear transfer with DIA per sweep, fully explicit computation of the nonlinear transfer with DIA per sweep, fully explicit computation of the nonlinear transfer with DIA per iteration, fully explicit computation of the nonlinear transfer with DIA per iteration, but neighboring interactions are interpolated in piecewise constant manner. Calculating the interactions per iteration instead of per sweep decreases the computing time but increases the amount of required memory with a factor of 1.5. In Hashimoto et al. (2003), it was demonstrated that the accuracy of the DIA may be improved by increasing the number of quadruplet configurations. They proposed a Multiple DIA with up to 6 wave number configurations.

3. MODEL PARAMETERIZATIONS AND COMPUTATIONAL STRATEGIES

The area considered has the origin with the coordinates (27.5°, 41.0°) and the lengths in x-direction (longitude) 14° and in y-direction (latitude) 6°, covering both the Black Sea and the Sea of Azov, as illustrated in Figure 1. In the geographical space the computational grid was chosen identical with the bathymetric grid and has 176 points in x direction and 76 points in y direction, with Δx=Δy=0.08°. In the direction-frequency space 24 directions and 30 frequencies were assumed. The computations were performed in the non stationary mode with a 20 min time step and the number of iterations was set from 1 which is the default value to 4 increasing in this way the numerical accuracy reached until the model passes to another time step.
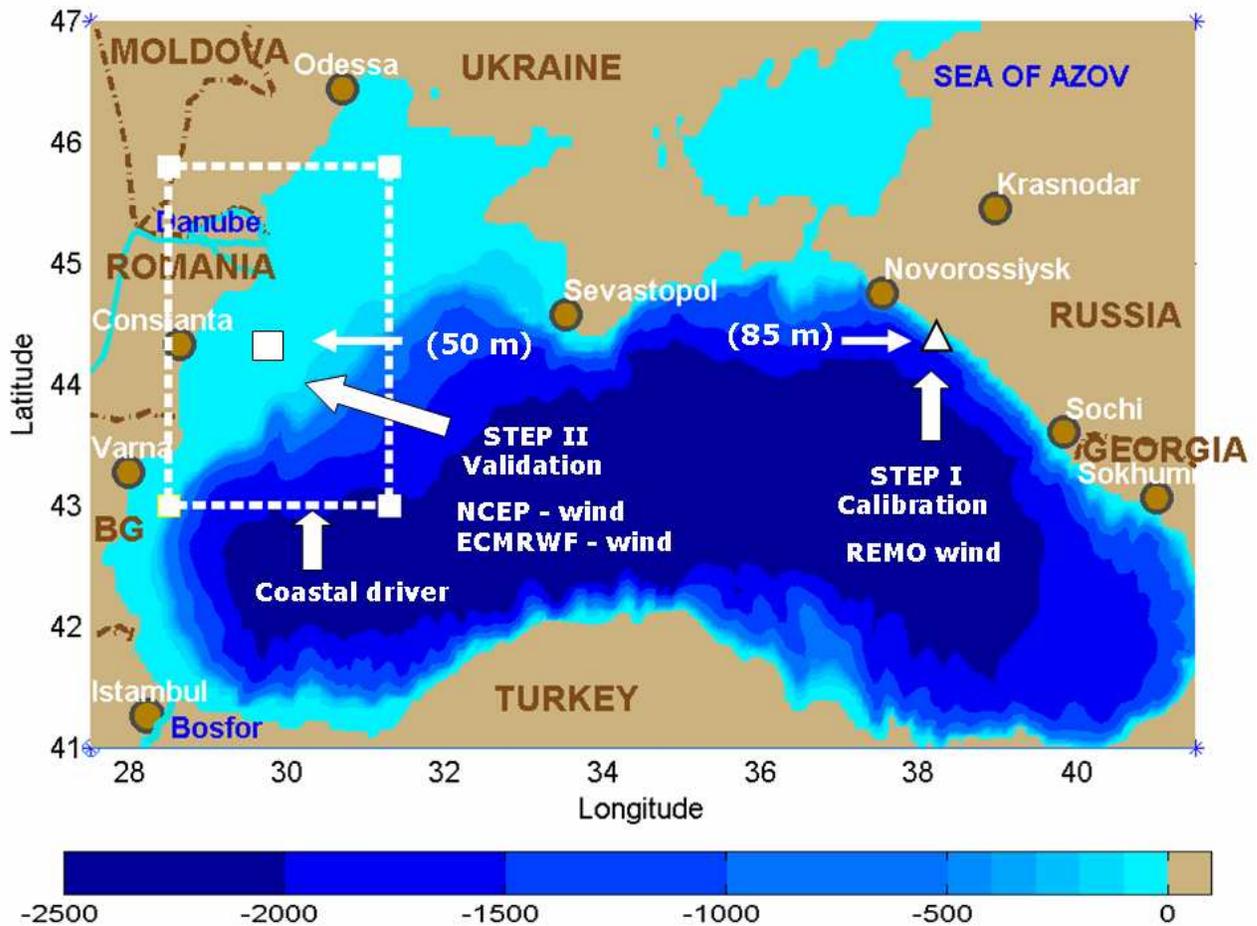

Figure 1: The bathymetric map of the Black Sea and the data sources.

The model implementation was achieved following two steps. In the first step model simulations were performed for the period 1st of November 1996 – 6th of February 1997. The wind field for this time interval was provided by the project HIPOCAS "Hindcast of Dynamic Processes of the Ocean and Coastal Areas of Europe", developed in the framework of the European Program "Energy, Environment and Sustainable Development", which gave the reanalysis wind conditions for 44 years, between 1958 and 2001, (Guedes Soares et al., 2002). For the wave simulations in the Black Sea, described here, the global NCEP reanalysis wind was used as a driver for the regional atmosphere model REMO. The spatial resolution of the wind model output was 0.25° and the time step of one hour. As a first checkpoint a directional buoy located into the north-east part of the Black Sea basin (37.98E, 44.51N) was used (illustrated in Figure 1). At that site the water depth is of 85m and the distance to shore is of about 7 kilometres.

At this level the model calibration was performed and all the possibilities for tuning SWAN were experimented. As regards the atmospheric input source term, presented in equation 2, two different options for the coefficient B are available corresponding to Komen's and respectively Janssen's formulations, while the linear growing term A has not a great impact in the wave growth. The simulations were performed however considering this linear growing term activated. In deep water wave modelling the weak link is considered the white-cap dissipation source term. This is derived from the Hasselmann pulse based model as described by equations (3) and (4). The coefficients in the steepness dependent coefficient Γ depend on the wind input formulation. Besides these two classical formulations the cumulative steepness method was also evaluated. The five options computationally viable for the quadruplet interactions were all assessed and will be discussed. WAM results corresponding to the same data set were also analyzed at this step.

In the second step two other different wind fields were used. These are NCEP (from the US National Centers for Environmental Prediction) with a spatial resolution of 1.875° and ECMRWF (from the European Centre for Medium-Range Weather Forecasts in UK) with a spatial resolution of 2.5°. For both fields the temporal resolution was of six hours. Simulations were performed for the period 1st of January 2002 – 31st of July 2002. Data measured at the Gloria drilling unit located cloase to the western coast of the Black Sea basin were used this time as reference.

4. EAST COAST CALIBRATION

Three different simulations were performed using the three parameterizations for white-capping dissipation available into the model, Komen, Janssen and CSM respectively, as discussed in the previous sections.

The default values of the tuneable coefficients were found inappropriate for the Black Sea conditions and after various calibrations these coefficients were set as follows: for Komen formulation $C_{ds} = 1.12 \times 10^{-5}$ (default 2.36×10^{-5}), for Janssen formulation $C_{ds1} = 1.1$ (default 4.5), and for CSM $C_{wc}^{st} = 0.1$ (default 0.5). In this way the dissipation by white-capping is reduced and as a consequence the wave height fields are increased. For the other physical processes the default parameterizations were used, that is the triad wave-wave interactions were not activated and for the quadruplet wave-wave interactions the fully explicit computations of the nonlinear transfer with DIA (Discrete Interaction Approximation) per sweep was used.

Table 1 presents the statistical results for the SWAN model simulations using the three parameterizations for white-capping Komen, Janssen and CSM, respectively. The period in analysis was between 1st November 1996 and 6th February 1997.

Table 1: Wave statistics concerning the whitecapping parameterization (1996.11.01h00-1997.02.06h00)

n=660	Bias	RMSE	SI	r	Case
Hs (m)	-0.008	0.386	0.384	0.871	K
Tp (s)	0.369	1.42	0.253	0.651	O
Dir (°)	8.58	53.5	0.25	0.47	M
Hs (m)	-0.022	0.432	0.430	0.837	J
Tp (s)	0.1	1.516	0.270	0.562	N
Dir (°)	-8.4	68.1	0.315	0.33	S
Hs (m)	-0.099	0.407	0.405	0.865	C
Tp (s)	-0.197	1.43	0.255	0.629	S
Dir (°)	-5.83	66.65	0.308	0.403	M

The statistical data analysis shows that the Komen formulation gives better results for all the three wave parameters compared (Hs, Tp and Dir). In this case all the indicators (RMSE, SI and r) have better values. Moreover this was the parameterization for which the smallest relative modification of the tuneable coefficient was necessary. The significant wave height

scatter plot corresponding to Komen's parameterization is presented in Figure 2.

The results were also compared with those provided by the WAM model for the same time interval at the end of 1996 and the beginning of 1997 that used exactly the same wind data field, Vlachev et al. (2004). It has to be noticed that the SWAN results are superior to that provided by WAM for any of the SWAN parameterization considered. Referring to the RMSE the values obtained were for Hs: 0.53, for Tp: 1.74 and for Dir: 92.7, which means higher root mean square errors at least as regards the significant wave height and the mean direction. The scatter indexes obtained were: 0.68 for Hs, 0.34 for Tp and 0.46 for Dir, which means also that the results of SWAN are better. Finally the computed correlation coefficients were for Hs: 0.73, for Tp: 0.55 and 0.36 for Dir. This means also better correlations with the measured data as concerns the SWAN results in comparison with WAM. However it must be noticed that the present implementation of SWAN used a discretisation of 30 frequencies while the WAM implementation only adopted 25 frequencies. The comparison would be more meaningful if the number of frequencies would be the same in both implementations.
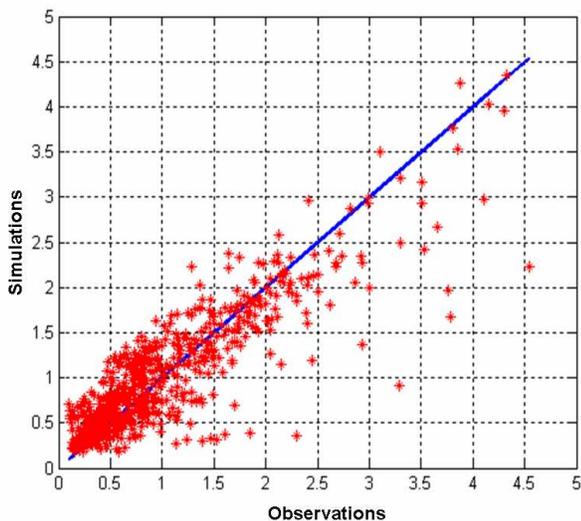

Figure 2: Hs scatter plot, Komen parameterization (1996.11.01h00 -1997.02.06h00), 660 data points (X axis – observations at the buoy, Y axis – SWAN simulations)

The second series of simulations were focused on the analysis of the influences of the quadruplet non linear interactions making a balance between the computational time and the accuracy of the results. Nine parameterizations are available in the SWAN model for the quadruplet interactions. Four of them are

based on the fully computation of the Boltzmann integral (FD-RIAM, Xnl for deep water transfer, Xnl for deep water transfer with WAM depth scaling and Xnl for finite depth transfer). However none of these formulations can be used operationally on a PC platform. The effectiveness of three different formulations based on the DIA approximation was assessed. These are: Q1- semi-implicit computation of the nonlinear transfer with DIA per sweep, Q2- fully explicit computation of the nonlinear transfer with DIA per sweep (default in SWAN) and Q3- fully explicit computation of the nonlinear transfer with DIA per iteration. The computations were performed on a Pentium IV PC platform with a 3 GHz processor and RAM memory of 384 MB. The statistical results and the corresponding computer times are presented in Table 2.

Table 2: Wave statistics concerning the quadruplet's parameterizations (1997.01.01h00-1997.02.06h00)

n=272	Bias	RMSE	SI	r	Case/ Time
Hs (m)	0,008	0,316	0,290	0,921	
Tp (s)	0,467	1,375	0,234	0,72	Q1
Dir (°)	20,36	51,657	0,225	0,58	22h26min
Hs (m)	-0,028	0,321	0,294	0,919	
Tp (s)	0,604	1,429	0,243	0,723	Q2
Dir (°)	22,643	51,344	0,223	0,602	14h10min
Hs (m)	-0,029	0,321	0,295	0,919	
Tp (s)	0,576	1,408	0,240	0,726	Q3
Dir (°)	22,676	51,712	0,225	0,591	16h45min

From the analysis of the data in the table 2 the results for the case Q1 are better in terms of *RMSE* and *SI* for the parameters Hs and Tp, as regards the directions however the results become better in the case Q2. For the case Q3 there are no better results for any of the parameters considered. From the computational point of view the default case Q2 seems to be the best.

Differences between wave model simulations and measurements can be generated due to various factors, most frequent being: differences between wind fields used for calculations from the real, inaccurate measurements and errors due to the choices of some parameters in the wave model (the default options being

not always the most appropriate for a specific area). Lopatoukhin et al. (2004) provided some interesting information concerning the wind and wave climate of the seas around Russia including the Caspian and Black Seas. Hence as regards the NCEP reanalysis wind the best correspondence is in the North (Barents Sea where the correlation was of about 0.9). However it seems also that this correlation decreases somehow when moving to the south direction.
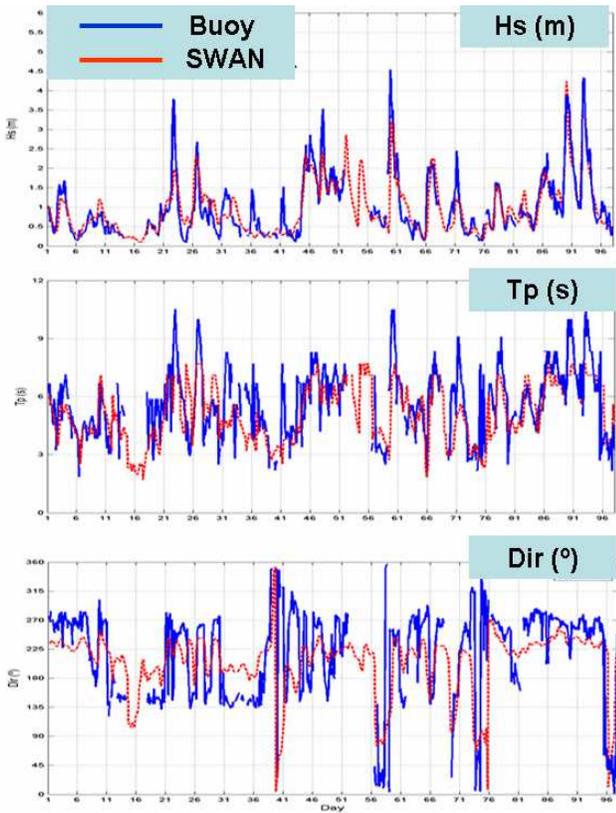

Figure 3: Direct comparison SWAN (Komen, modified 2 parameters) buoy, day 1 - 1996.11.01, day 96- 1997.02.04

In the same work some results were presented concerning simulations with the SWAN model (version 40.31) in the Caspian Sea. The simulations were made only using the Komen parameterization and various values were tested for the coefficients C_{ds} and $\tilde{S}_{PM}^2$ (from the default values 2.36×10^{-5} and 3.02×10^{-3} till the values 1.86×10^{-5} and 3.62×10^{-3}), actually following the same path for calibrating the model as in the present work. Following their results an additional simulation was performed considering the Komen parameterization and the values $C_{ds} = 1.36 \times 10^{-5}$ and $\tilde{S}_{PM}^2 = 3.62 \times 10^{-3}$ for the tunable coefficients. The direct comparisons with the buoy data are presented in Figure 3. No significant differences with respect to the previous simulations were encountered in statistical terms.

A more detailed description of this SWAN model calibration in the east coast of the Black Sea is given in Guedes Soares and Rusu (2005).

5. WEST COAST VALIDATION

In the second step, model simulations were performed in order to validate the wave prediction system also on west coast of the Black Sea.

Usually the west side of the sea is more energetic. That is why first a brief analysis of some in situ data measured on the west side, at the Gloria drilling unit (about 50 meters water depth), for the period 2001- 2005, was performed bellow. The location of this drilling unit considered as reference is illustrated in Figure 1.

In terms of significant wave heights and wave periods the average and maximum values corresponding to each month as registered at the Gloria drilling unit in the time interval 2001-2005 are presented in Figure 4a and 4b, while the global distribution of wave directions in percents is illustrated in Figure 4c.
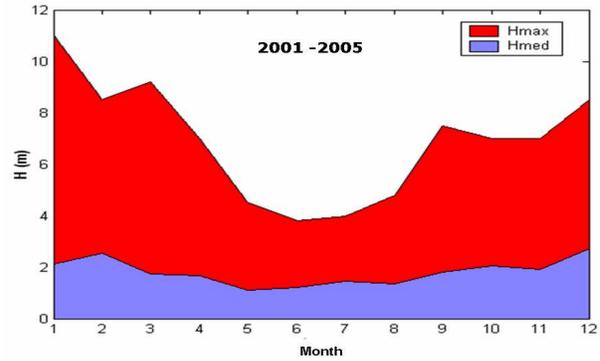

Figure 4a: Hs monthly average and maximums in the time interval 2001-2005 registered at the Gloria unit.
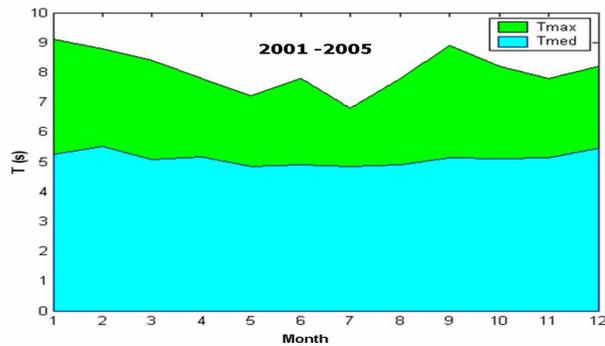

Figure 4b: Monthly average and maximums for the wave period in the time interval 2001-2005 as registered at the Gloria unit.
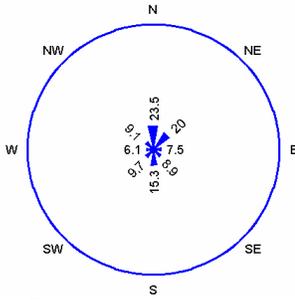
Figure 4c: Global percents distribution of wave directions in the time interval 2001-2005, registered at the Gloria unit.

At this second level two wind fields were used: NCEP (1.875º spatial resolution) and ECMRWF (2.5º spatial resolution), the temporal resolution of both fields was of 6 hours while the time interval considered was 1st of January 2002 – 31st of July 2002. Data measured in situ at the Gloria driling unit were used as reference at this stage. The unit is located in the western coastal environment of Black Sea (about 50m water depth) and both wind and wave measurements were available.

First a comparison between the measured wind velocities versus the predictions coming from the two different model systems was made. The measurements of the wind velocities have been performed at 28 meters height and the wind speeds were adjusted from 28 to 10 meters using the simple relationship from Hsu et al. (1994)

$$u_2 = u_1 \left(z_2 / z_1 \right)^P \qquad (8)$$

where u_2 denotes the wind speed at the reference height (28 meters), z_2, and u_1 represents the wind speed measured at height z_1 (10 meters). The exponent, P, is set to 0.11 based on an empirical relationship for typical sea conditions. The direct comparison between the measured and predicted wind velocities is presented in Figure 5 while the statistical results in Table 3.
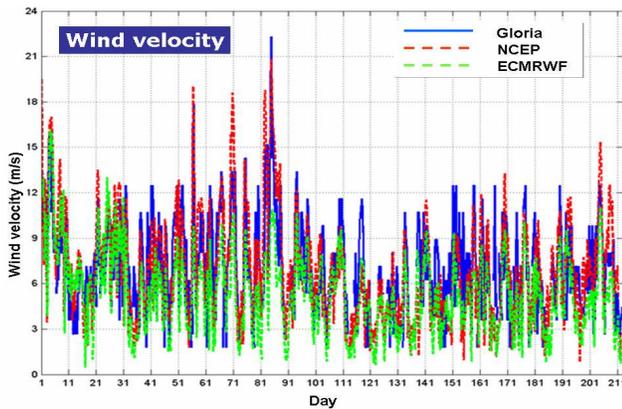

Figure 5: Direct comparison for wind velocity: GLORIA (measured) - NCEP – ECMRWF, day 1 – 2002/01/01, day 211 – 2002/07/31

Table 3: Wind statistics using the measurements at Gloria unit as reference (2002.01.01-2002.07.31)

n= 781	Bias	RMSE	SI	r	Wind field
Vw (m/s)	0,848	3,11	0,396	0,621	NCEP
	2,38	3,48	0,444	0,675	ECMRWF

The above statistical results show that the wind velocities coming from the atmospheric models are systematicaly smaller than the measurements (positive biases) and the NCEP wind fields are usualy closer to the measurements.

SWAN simulations were performed considering the model parametrization defined in the previous section and the two different wind fields. In terms of significant wave height the direct comparison between the model results and the measurements is illustrated in Figure 6. The statistical results are presented in Table 4
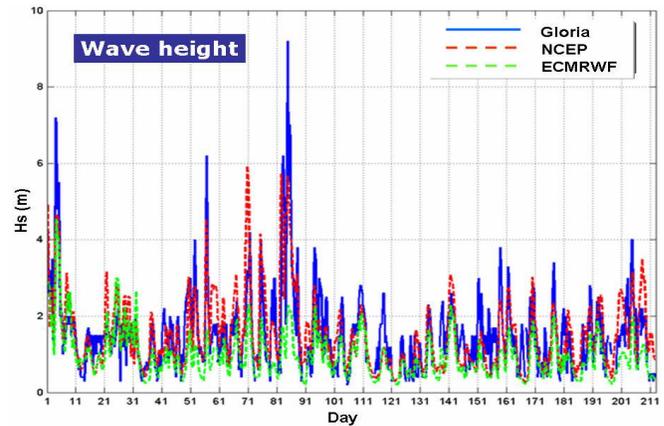

Figure 6: Comparison for significant wave height: GLORIA (measured) – SWAN (NCEP) – SWAN (ECMRWF), day 1 – 2002/01/01, day 211 – 2002/07/31

Table 4: Wave statistics using the measurements at Gloria unit as reference (2002.01.01-2002.07.31)

n=781	Bias	RMSE	SI	r	Wind field
Hs (m)	-0,016	0,762	0,496	0,709	
Tm (s)	2.342	2.664	0.524	0.218	NCEP
Dir (°)	74,05	81,08	0,377	0,401	
Hs (m)	0,539	0,937	0,610	0,683	
Tm (s)	2,731	2,972	0,585	0,300	ECMRWF
Dir (°)	81,407	87,133	0,405	0,341	

As expected, the results using the NCEP wind field are better than those provided when the ECMRWF wind field is used. However they are less accurate than for the case discussed in the previous section when the wind resolution was higher both in space and time.

An important aspect refers to the high energetic conditions when the wave height peaks seem to be systematically underestimated by the model. One solution that is taken into account is to define another model parameterization special for this highest energetic cases and the work is still ongoing in this direction.

6. THE BLACK SWAN WAVE PREDICTION SYSTEM

As discussed in the introductory part, the main advantage of using SWAN for wave generation is that the system can be easily extended into the nearshore direction. Some features of the system designed, having the generic name Black Swan, will be presented in this section.

The first step was to develop the nearshore connection for the wave prediction system and this was accomplished by defining 10 sectors for covering in this way the entire coastal environment of the Black Sea basin. These coastal drivers are illustrated in Figure 7 and all of them have been already implemented. After case other coastal domains can be also considered.

The second step concerns the coastal focusing and an example is given in Figure 8 for the west coast side.

The west coast is usually the most energetic area of the Black Sea and the case presented in Figure 8 refers to a strong storm corresponding to the time frame 2002/03/11/h18.

As illustrated in the figure above the system focalization assumes four levels: level I corresponding to the generation area, level II for the coastal transformation, level III for local focusing and level IV for high resolution simulations using Cartesian coordinates. For the case illustrated in Figure 8 the characteristics of the computational grids are presented in Table 5.

Table 5: Computational grids characteristics

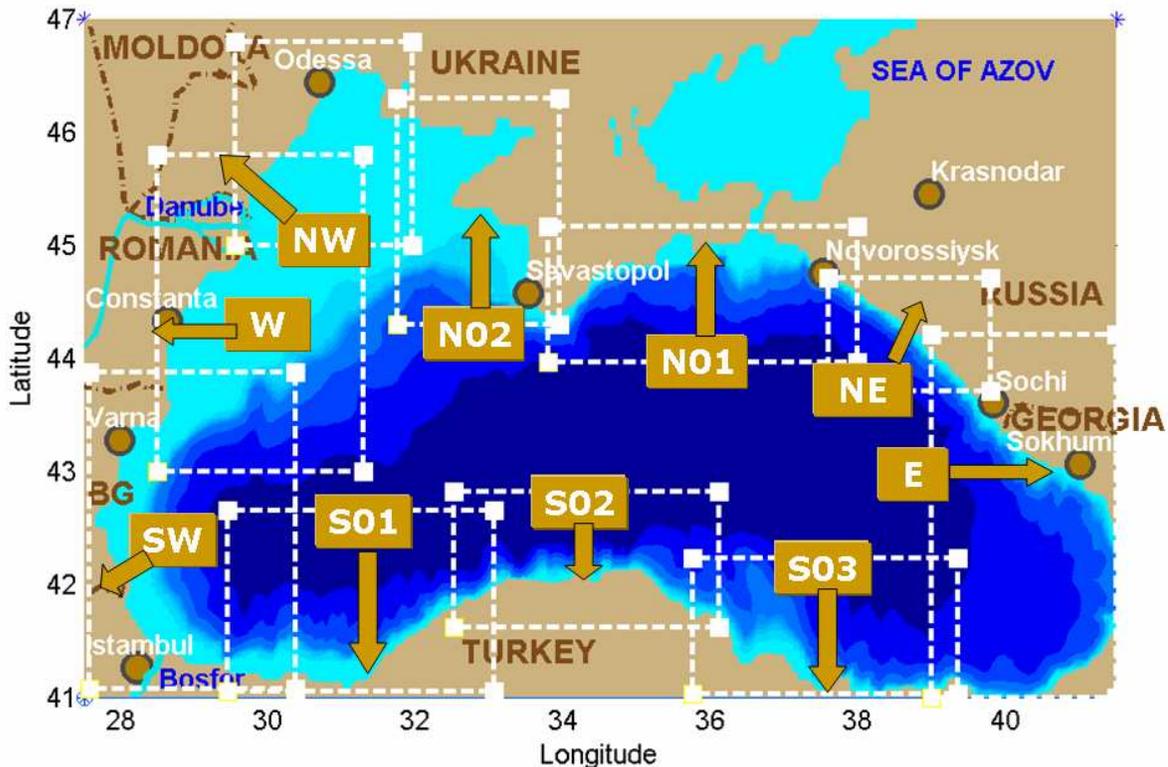| Grids	$\Delta x \times \Delta y$	Δt min	nf	nθ	ngx $\times$ ngy = np
Global	0.08° × 0.08°	20	30	24	176 × 76 = 13376
Coastal	0.02° × 0.02°	20	30	36	141 × 141 = 19881
Local	0.005° × 0.005°	20 or st	30	36	161 × 141 = 22701
Cartesian	50m × 50m	st	25	36	96 × 107 = 10272

Figure 7: The nearshore connection for the wave prediction system (definition of 10 coastal drivers).
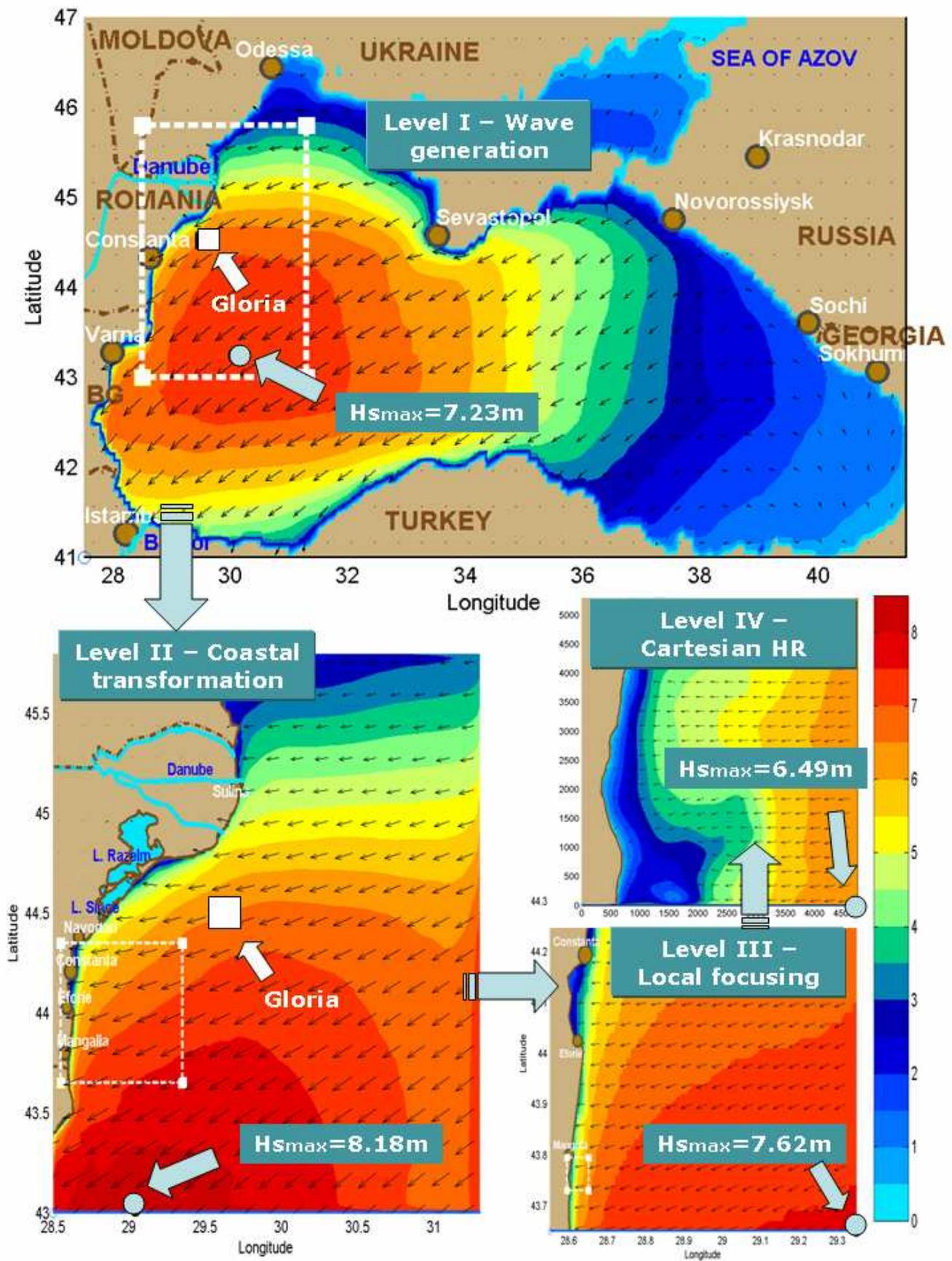
Figure 8: West coast focusing of the wave prediction system, significant wave height fields and wave vectors corresponding to time frame 2002/03/11/h18, storm case.

At this point a brief discussion will be made in relationship with the system focusing towards nearshore in general and the case presented in Figure 8, which is a typical storm case, in particular. For the global and coastal areas the non stationary mode is in general required, and a 20 minutes time step seems to be effective. However, the numerical schemes used are different, while the global area uses the second order scheme S&L characteristic for large areas in non stationary mode, in the case of the coastal areas the BSBT scheme (backward space backward time) was applied. The importance of the coastal driver is illustrated in Figure 8 where can be seen that, due to the local effects, an increase of almost one meter in terms of maximum significant wave height was encountered for the case studied when passing from the generation area to the nearshore transformation.

The next two areas are in shallow water, hence the total source term is expressed by the equation (9).

(9)

$$S_{total} = S_{in} + S_{dis} + S_{nl} + \underbrace{S_{bf} + S_{brk} + S_{tri} + ...}_{Finite\ depth\ processes}$$

Besides the three source terms discussed before for deep water, additional source terms corresponding to phenomena like bottom friction, depth induced breaking and triad non linear wave-wave interactions may play an important role. For the levels II and III the standard SWAN nesting procedure was applied with a ratio of increasing resolution of 4, as shown in Table 5. For the last level when passing from spherical to Cartesian coordinates the coupling with the previous level was achieved by providing variable boundary conditions on the active boundaries (in the case illustrated in Figure 8 these boundaries are North, East and South). While for the level III the non stationary mode can alternate with stationary simulations for the last level seems to be in general more convenient to use only the stationary mode.

There are two reasons for passing in the case of this last level from spherical to Cartesian coordinates. One is that in SWAN model some processes as diffraction or wave set up are working better in Cartesian coordinates. The second is that in this way can be made a simpler link with surf models (SHORECIC for example) that work in a Cartesian reference system.

A user friendly interface in the form of a Matlab toolbox has been associated to this wave prediction system. Besides pre and post processing the computational environment developed provides visualization facilities of the model input and output as illustrated in the Figures 1, 7 and 8. Interactions with MMAP toolbox were also developed for quick

coordinate transformations.

7. FINAL CONSIDERATIONS

A wave prediction system based on the SWAN model was designed for the Black Sea basin. The effectiveness of various deep water parameterizations was evaluated and under certain limitations the model system can provide reliable information concerning the wave climate in the Black Sea basin and the nearshore wave impact.

Using the same model to cover almost the full scale from the wave generation, passing through the nearshore transformation and close to the surf zone, a flexible system with the capacity to focalize quickly on any coastal area of the Black Sea was designed. A Matlab toolbox was associated to the computational environment as an effective instrument for a quick implementation of successive areas as well as for comprehensive data visualization.

Various data sources will be further considered in order to continue the validation of the present wave prediction system at different scales both in space and time frames.

As shown in the sections 4 and 5 the influence of the accuracy of the wind field is a problem of extreme importance for an adequate prediction of the wave climate. In this connection, the uncertainties in the atmospheric models still remain a major problem especially as concerns very strong storms.

8. ACKNOWLEDGEMENTS

9. REFERENCES

Cavaleri, L. and P. Malanotte-Rizzoli, 1981: Wind wave prediction in shallow water: Theory and applications. *J. Geophys. Res.*, **86**, No. C11, 10,961-10,973.

Divinsky, B.V., Levin, B.V., Lopatukhin, L.I., Pelinovsky, E.N. and Slyunyaev, A.V., "A freak wave in the Black Sea: observations and simulation", *Doklady Earth Sciences*, 2004, 395A, pp. 438 - 443.

Guedes Soares, C., Weisse, R., Carretero J.C. & Alvarez, E., 2002: A 40 years Hindcast of Wind, Sea Level and Waves in European Waters, *Proceedings of the 21st International Conference on Offshore Mechanics and Arctic Engineering (OMAE'02),* ASME Paper OMAE2002-SR28604.

Guedes Soares, C. and Rusu, E., 2005: SWAN hindcast in the Black Sea, *Proceedings Fifth International Symposium on Ocean Wave Measurement and Analysis (WAVES 2005),* Madrid, Spain, 3rd-7th July 2005, CD edition, 9p.

Hashimoto, N., H. Tsuruya and Y. Nakagawa, 1998: Numerical computations of the nonlinear energy transfer of gravity-wave spectra in finite water depths, *Coastal Engng. J.*, **40,** 23-40.

Hashimoto, N., IJ.G. Haagsma and L.H. Holthuijsen, 2003: Four-wave interactions in SWAN, *Proc.28th Int. Conf. Coastal Engng.*

Hasselmann, K., 1974: On the spectral dissipation of ocean waves due to white-cap, *Bound.-layer Meteor.*, **6**, 1-2, 107-127.

Hasselmann, S., K. Hasselmann, J.H. Allender and T.P. Barnett, 1985: Computations and parameterizations of the nonlinear energy transfer in a gravity wave spectrum. Part II: Parameterizations of the nonlinear transfer for application in wave models, *J. Phys.Oceanogr.,* **15,** 11, 1378-1391.

Hsu, S.A., E.A. Meindl, and D. Gilhousen, 1994: Determining the Power-Law Wind-Profile Exponent under Near-Neutral Stability Conditions at Sea, *J. App. Met*, **33**(6).757-765.

Hurdle, D.P. and G. Ph. van Vledder, 2004: Improved spectral wave modelling of white-capping dissipation in swell sea Systems. *Proc. 23rd Int. Conf. on Offshore Mech. and Arctic. Eng, OMAE2004*

Janssen, P.A.E.M., 1989: Wave induced stress and the drag of air flow over sea waves*, J. Phys.Oceanogr.,* **19**, 745-754.

Janssen, P.A.E.M., 1991: Quasi-linear theory of wind-wave generation applied to wave forecasting, *J. Phys. Oceanogr.,* **21**, 1631-1642.

Komen, G.J., S. Hasselmann, and K. Hasselmann, 1984: On the existence of a fully developed wind sea spectrum, *J. Phys. Oceanogr.,* 14, 1271-1285.

Lopatoukhin, L.J., Boukhanovsky, A.V., Chernysheva, E.S., Ivanov, S.V., 2004: Hindcasting of wind and wave climate of seas around Russia, Proc. the 8th *International Workshop on Waves Hindcasting and Forecasting, North Shore,* Oahu, Hawaii, November 14-19.

Miles, J.W., 1957: On the generation of surface waves by shear flows, *J. Fluid Mech.,* **3**, 185-204.

Phillips, O.M., 1957: On the generation of waves by turbulent wind*, J. Fluid Mech.,* **2,** 417-445.

Resio, D.T., J.H. Pihl, B.A. Tracy and C.L. Vincent, 2001: Nonlinear energy fluxes and the finite depth equilibrium range wave spectra, *J. Geophys. Res.*, **106**, C4, 6985-7000.

Snyder, R.L., Dobson, F.W., Elliott, J.A. and R.B. Long, 1981: Array measurement of atmospheric pressure fluctuations above surface gravity waves, *J. Fluid Mech.,* 102, 1-59.

Tolman, H.J., 1992: Effects of numerics on the physics in a third-generation wind-wave model, *J.Phys. Oceanogr.,* **22**, 10, 1095-1111.

Valchev, N., Pilar, P., Cherneva, Z. and Guedes Soares, C., 2004: Set-up and validation of a third-generation wave model for the Black Sea*, Proc. 7th Int. Conf. "BLACK SEA'2004",* Scientific and Technical University of Varna. Bulgaria, 273-279.

Van Vledder, G. Ph. and M. Bottema, 2003: Improved modelling of nonlinear four-wave interactions in shallow water, *Proc. 28th Int. Conf. Coastal Engineering*, ASCE, 459-471

WAMDI group, 1988: The WAM model - a third generation ocean wave prediction model, *J. Phys. Oceanogr.,* **18**, 1775-1810.